ACS Synthetic Biology

pubs.acs.org/synthbio Research Article

Engineering Transcription Factor XylS for Sensing Phthalic Acid and Terephthalic Acid: An Application for Enzyme Evolution

Jiawei Li,‡ Mario Roque Huanca Nina,‡ Xiaoyan Zhang,‡ and Yunpeng Bai*

Cite This: *ACS Synth. Biol.* 2022, 11, 1106−1113 Read Online

ACCESS | Metrics & More | Article Recommendations | Supporting Information

ABSTRACT: Poly(ethylene terephthalate) (PET) and phthalate esters (PAEs) are used extensively as plastics and plasticizers. Enzymatic degradation of PET and PAEs has drawn great attention in recent years; however, evolution of PET- and PAE-degrading enzymes is still a big challenge, partly because of the lack of an effective screening method to detect phthalic acid (PA) and terephthalic acid (TPA), which are the main hydrolysis products of PAEs and PET. Here, by directed evolution of a promiscuous transcription factor, XylS from *Pseudomonas putida*, we created two novel variants, XylS-K38R-L224Q and XylS-W88C-L224Q, that are able to bind PA and TPA and activate the downstream expression of a fluorescent reporter protein. Based on these elements, whole-cell biosensors were constructed, which enabled the fluorimetric detection of as little as 10 μM PA or TPA. A PAE hydrolase, *Go*Est15, was preliminarily engineered using this new biosensor, yielding a mutant *Go*Est15-V3 whose activity toward dibutyl phthalate (DBP) and *p*-nitrophenyl butyrate was enhanced 2.0- and 2.5-fold, respectively. It was shown that 96.5% DBP (5 mM) was degraded by *Go*Est15-V3 in 60 min, while the wild-type enzyme degraded only 55% DBP. This study provides an effective screening tool for directed evolution of PAE-/PET-degrading enzymes.

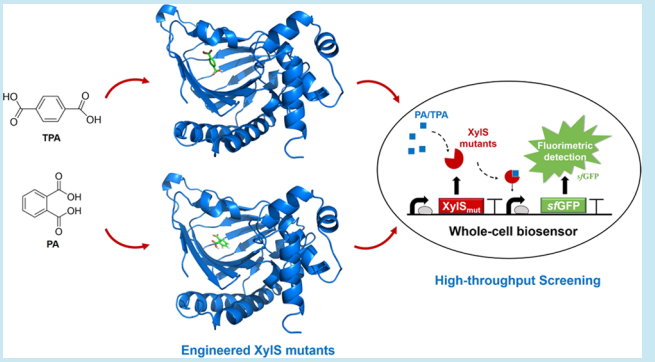

KEYWORDS: *biosensor, transcription factor engineering, phthalic acid, terephthalic acid, enzyme evolution, biodegradation*

INTRODUCTION

Poly(ethylene terephthalate) (PET) and phthalate esters (PAEs) are widely used as consumer plastics and industrial plasticizers, respectively. Their hydrolysis rates are remarkably slow in the natural environment, which results in serious concerns regarding pollution and public health.[1−7] Terephthalic acid (TPA) and phthalic acid (PA) are the main building blocks and hydrolysis products of PET and PAEs, respectively; both are industrially produced from raw petroleum. Detection of TPA and PA can indicate the degree of degradation of PET and PAEs. There are many reports about biodegradation of PET and PAEs,[8−15] but low enzyme activity toward these persistent and chemically inert materials impedes real-world applications. Structure-based and computational-aided protein engineering of PET-degrading enzymes have been applied to improve their catalytic performance.[10,16−19] These approaches rely on the elucidation of enzyme three-dimensional (3D) structures and mechanistic insights.[16,20−23] However, because of the lack of feasible screening methods to detect PA/TPA, the power of directed evolution has not been fully exploited.

High-performance liquid chromatography (HPLC) can be used to detect and quantify trace amounts of TPA/PA, but this time-consuming and discontinuous assay is not suitable for rapid screening of protein libraries that usually contain 10^5−10^7 variants.[24] The fluorimetric assay is a sensitive tool for product detection, but PA and TPA are not fluorescent. TPA can be converted to hydroxyphthalic acid, which can be detected by measuring fluorescence at 421 nm,[25−27] but the addition of Fe(II) and H_2O_2 is not favorable for enzymes and this approach is thus unsuitable for large-scale screening. Furthermore, this method cannot be used to detect PA.

Transcription factor (TF)-based whole-cell biosensors provide a flexible protocol that couples detection of target molecules with the downstream expression of fluorescent reporter proteins, enabling the fluorimetric detection of molecules and screening of protein variants.[28−32] Detection using whole-cell biosensors relies on the binding of target molecules to TFs. To date, many TFs have been identified as recognizing various small molecules.[33−37] TphR from *Comamonas* sp. strain E6 can bind TPA and regulate the expression of TPA metabolic pathway genes.[38] PobR was

Received: June 16, 2021
Published: February 22, 2022

https://doi.org/10.1021/acssynbio.1c00275
ACS Synth. Biol. 2022, 11, 1106−1113

Scheme 1. Fluorimetric Detection of PA and TPA Using Engineered XylS-Based Whole-Cell Biosensors

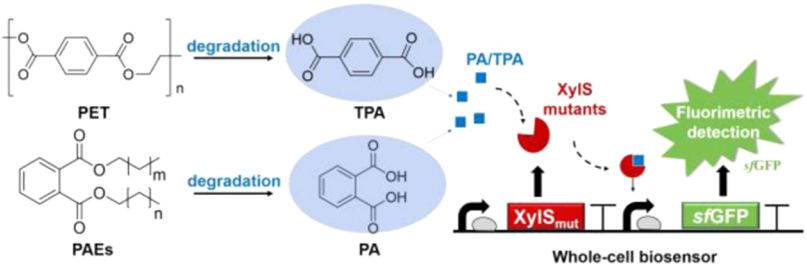

found to respond to *p*-hydroxybenzoate (*p*HB),[39] a TPA analogue, and its mutant can sense *p*-nitrophenol (*p*NP).[40] Thus, engineering TFs for sensing various chemicals has drawn great attention in microbial biotechnology.[41]

XylS is a promiscuous transcription factor from *Pseudomonas putida*.[42−45] It can bind benzoic acid and various derivatives, but it cannot recognize PA and TPA. Here, we attempted directed evolution of XylS to generate new TFs that are capable of binding and responding to TPA and PA (Scheme 1). Such XylS mutants could be used to construct whole-cell biosensors for fluorimetric detection of PA and TPA.

RESULTS AND DISCUSSION

Generation of the Wild-Type Biosensor *Escherichia coli*-pUC57-XylS-*sf*GFP. First, the *xylS* gene, the promoter Pm, and a green fluorescent protein-encoding gene (*sf*GFP) were recombined into plasmid pUC57. The resultant plasmid was transformed into *E. coli* BL21 (DE3) cells to generate the whole-cell biosensor *E. coli*-pUC57-XylS-*sf*GFP (Figure S1). Fluorescence analysis showed that this biosensor can detect 2-hydroxybenzoic acid and 3-chlorobenzoic acid, which are both known inducers of XylS, but the fluorescence did not change when TPA or PA were added to the cells (Figure S2).

Directed Evolution of XylS for Detecting PA and TPA. The mutation A111V was previously found to change the induction specificity of XylS.[46] Thus, the influence of residue 111 was investigated here by performing site-directed saturation mutagenesis. After screening, XylS variants A111C, A111L, A111V, and A111F showed clear fluorescence response to 5 mM PA and TPA (Figure S3). At 4 h, the fluorescence of XylS-A111V and A111F biosensor increased 3.3- and 2.7-fold compared with the blank control (0 mM), respectively, while the fluorescence of the wild-type biosensor did not increase significantly (Figure 1). These results showed that residue 111 was a switch for substrate specificity. Although mutation A111V can introduce the function of sensing 5 mM PA and TPA, the dynamic range and detection limit in low concentrations (0.1−2.5 mM) were not good enough (Figure 2).

To further improve the detection of PA and TPA by XylS mutants, error-prone polymerase chain reaction (PCR) was applied, and the generated libraries of XylS mutants were screened in 96-well plates. By comparing the fluorescence differences of cells induced by 0.5 mM PA/TPA with cells without induction, four variants were then rescreened in shaken flasks (Figure S4a). Among them, XylS-L224Q was the best mutant for the detection of 0.01−5 mM PA/TPA (Figure S4b,c). Then, the combined variant XylS-A111V-L224Q was subjected to a second round of random mutagenesis. XylS-K38R-W88C-A111V-N138I-L224Q was identified, and the detection of TPA by this mutant was improved in the range

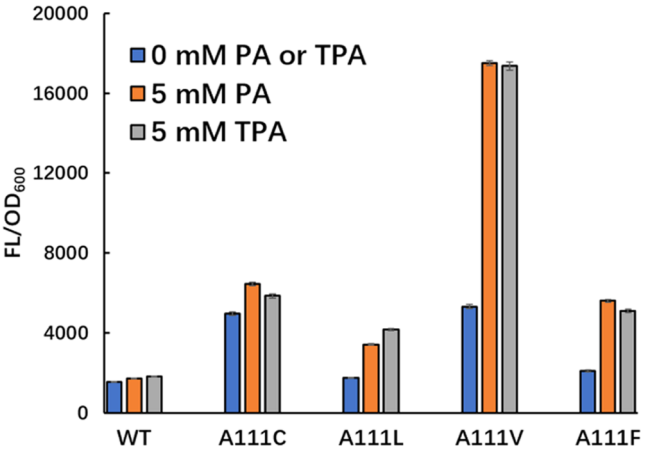

Figure 1. XylS site-directed saturation mutagenesis and its effect of some variants for detecting 5 mM PA and TPA at 4 h. Each experiment was carried out in three triplicates.

0.1−2.5 mM compared with XylS-A111V (Figures S5 and 2b). Then, three new mutations in this variant (i.e., K38R, W88C, and N138I) were decoupled and recombined to generate 19 variants with different combinations of point mutations (Table S1). Among them, the fluorescence differences of whole-cell biosensors containing XylS-K38R-L224Q and Xyls-W88C-L224Q were improved between 0 and 2.5 mM PA/TPA compared with the wild-type biosensors (Figure S6). In this range, the fluorescence of XylS-K38R-L224Q and XylS-W88C-L2224Q-based biosensors gradually increased 1.6- and 2.2-fold compared to the background (0 mM), respectively (Figure 2a). For 0−2.5 mM TPA, the fluorescence ratio of XylS-W88C-L2224Q-based biosensor was also increased 2.4-fold (Figure 2b). Compared with the wild-type XylS and XylS-A111V, the introduction of K38R-L224Q and W88C-L224Q mutations reduced the detection limit of PA/TPA to 0.1 mM (Figure S6a,d), validating our hypothesis that the substrate specificity of the promiscuous XylS can be modified. Notably, the initial mutation A111V did not appear in these mutants, showing that residue Ala-111 is not the sole switch for substrate change. Specificity switch was also observed in engineering the transcription factor PobR for detecting *p*NP.[40] Jha et al. showed that directed evolution of PobR led to a mutant pNPmut1 that can sense *p*NP as low as 2 μM, switching the specificity of the native effector *p*HB to *p*NP.[40] *p*HB is also a TPA analogue; however, it is not clear if this PobR mutant can sense TPA and PA. In this study, we showed that XylS mutants can respond to TPA/PA with the detection limit of 0.1 mM. Thus, it is reasonable to assume that engineering of TFs such as PobR may also generate new TPA/PA binding TFs with even lower detection limits.

https://doi.org/10.1021/acssynbio.1c00275
ACS Synth. Biol. 2022, 11, 1106−1113

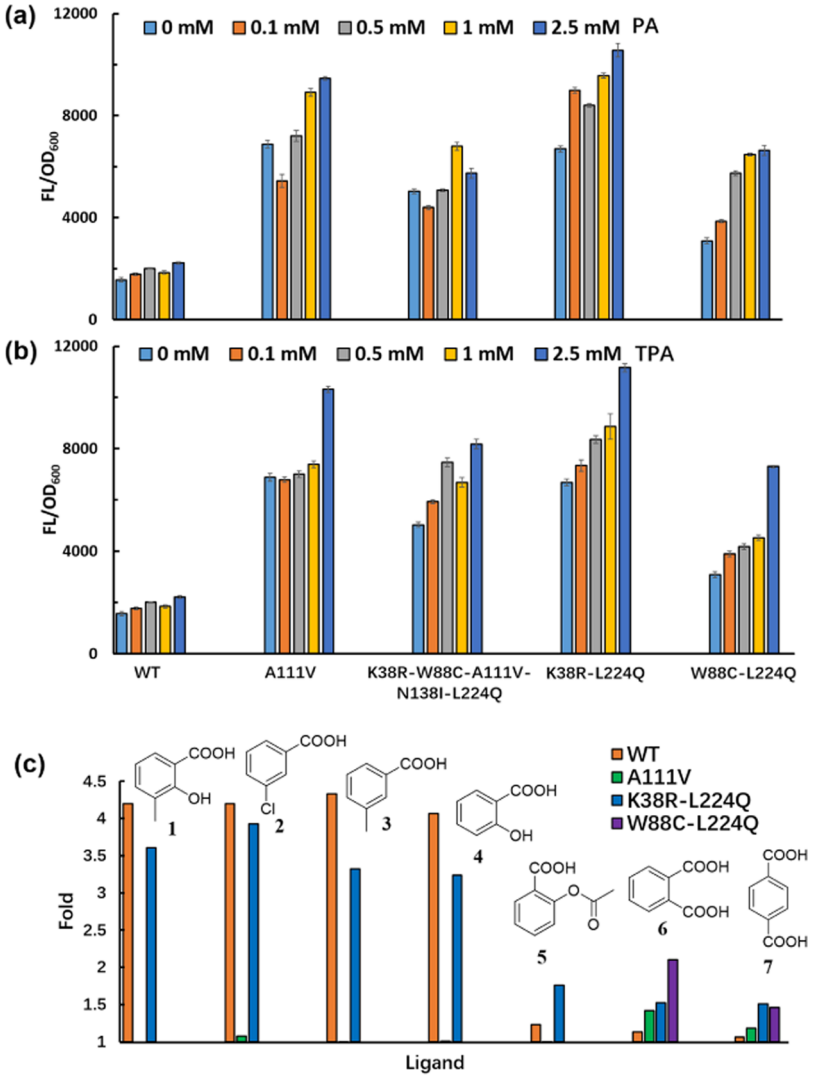

Figure 2. Fluorescence of whole-cell biosensors containing different XylS variants in response to (a) PA and (b) TPA at 2 h (4 h for XylS-K38R-W88C-A111V-N138I-L224Q) after induction. Each experiment was carried out in three triplicates. (c) Ligand specificity of the wild-type and engineered XylS. Fluorescence ratio of 1 mM each ligand to the background fluorescence at 4 h (2 h for K38R-L224Q and W88C-L224Q) after induction. **1**: 2-hydroxy-3-methylbenzoic acid, **2**: 3-chlorobenzoic acid, **3**: 3-methylbenzoic acid, **4**: 2-hydroxybenzoic acid, **5**: 2-acetoxybenzoic acid, **6**: PA, and **7**: TPA.

Characterization of the XylS Variant-Based Whole-Cell Biosensors. We then investigated the use of wild-type and engineered biosensors to detect different benzoic acid derivatives (Figures S7 and S8). After engineering, the ligand specificity of XylS was changed (Figure 2c). The wild-type biosensor showed higher fluorescence in response to ligands **1**−**4** compared with **5**−**7**. The K38R-L224Q-based biosensor maintained the relatively higher fluorescence toward **1**−**4** (although decreased compared with the wild-type biosensor), but its fluorescence response toward **5**−**7** increased clearly. This biosensor displayed a good dynamic range for detection of **1**, **2**, and **3** with detection limits of 1 μM. It can also detect 0.1 mM **4** and 0.5 mM isophthalic acid. Notably, although A111V increased the fluorescence toward 5 mM PA and TPA, its detection ability toward **1**−**5** was lost.

E. coli cells with XylS-K38R-L224Q and XylS-W88C-L2224Q-based *sf*GFP reporter systems were harvested at different time periods and studied using a confocal fluorescence microscope (Figure 3a). The wild-type biosensor cells showed no fluorescence at 0 h and only a few individual cells were fluorescent at 1 and 2 h due to leaky expression of the *sf*GFP gene (Figure 3a, column 1). When 0.5 mM PA or TPA was added, the number of fluorescent cells and their fluorescence intensities were similar to those of the wild-type biosensor at 1 and 2 h (columns 2 and 3), demonstrating that wild-type XylS cannot recognize PA or TPA. However, when 0.5 mM PA was added, the number of fluorescent cells containing XylS-K38R-L224Q and their fluorescence intensities were increased significantly compared with those of the wild-type biosensor at 1 and 2 h (Figure 3a, column 5). For the XylS-W88C-L224Q biosensor, when 0.5 mM TPA was added, the fluorescence intensities from single cells were much higher than those from the wild-type biosensor or cells without the addition of TPA (columns 6 and 7). These results were consistent with the measurements carried out in shaken flasks.

Next, we used fluorescence-activated cell sorting to analyze the fluorescence of large populations of cells (Figure 3b−d). For the wild-type biosensor, the distribution of the fluorescence intensity of the cells did not change much when 0.1−5 mM PA was added (Figure 3b). For the XylS-W88C-

https://doi.org/10.1021/acssynbio.1c00275
ACS Synth. Biol. 2022, 11, 1106−1113

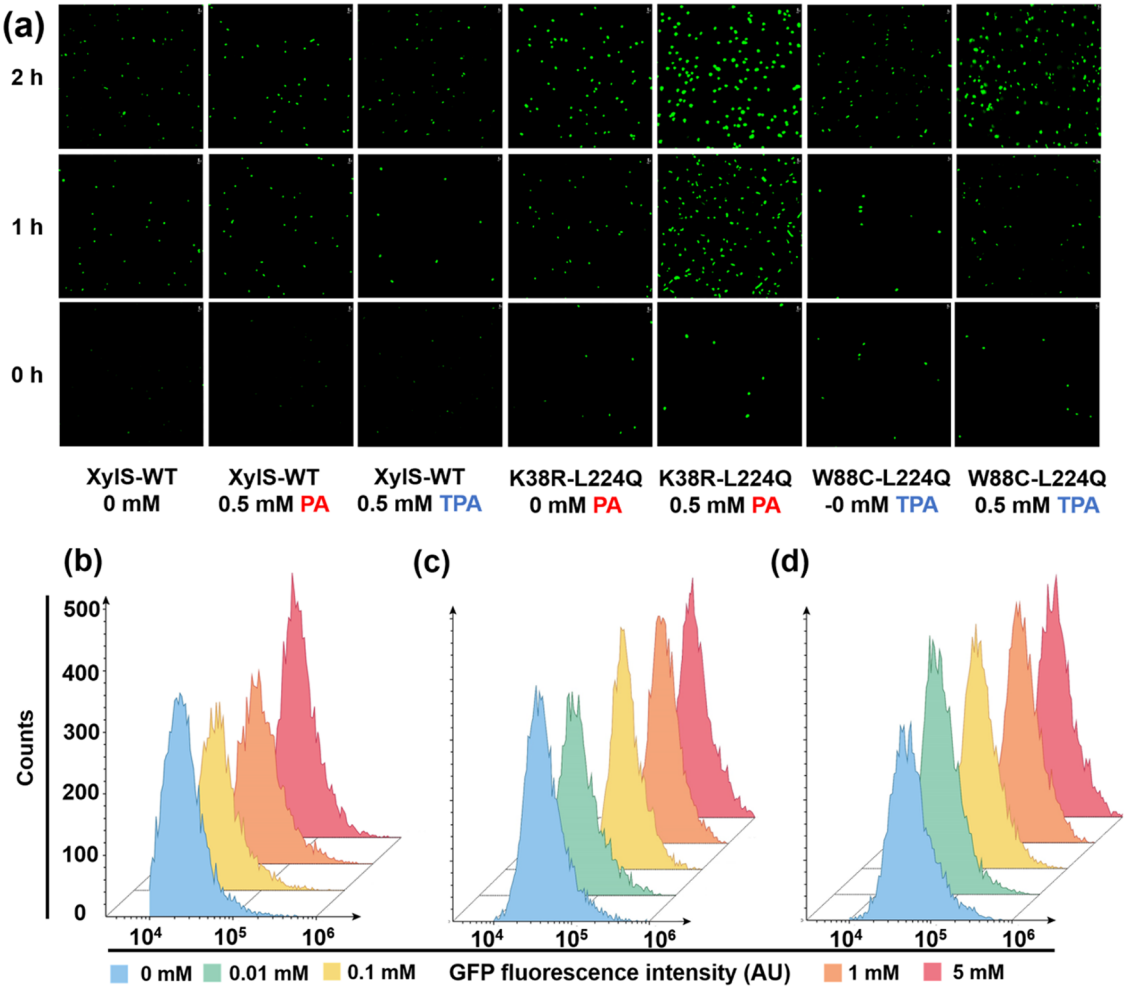

Figure 3. Single cell analysis of the evolved XylS biosensors. (a) Fluorescence images of biosensors in the presence of PA and TPA of different concentrations. Fluorescence characterization of (b) XylS, (c) XylS-K38R-L224Q with the induction of PA, and (d) XylS-W88C-L224Q with the induction of TPA.

L224Q- and XylS-W88C-L224Q-based biosensors, the proportion of cells with high fluorescence increased and the peaks clearly shifted toward the higher fluorescence field when 10 μM to 5 mM PA or TPA was added to the respective cell cultures (Figure 3c).

In the above experiments, we observed a relatively high background fluorescence (Figure 2) and leaky expression of the reporter gene in the engineered biosensors (Figure 3). To decrease this background fluorescence, the plasmid backbone was changed from a high copy number pUC57 to a low−medium copy number pCL1920 without changing the gene components. After plasmid replacement, the background fluorescence was decreased from 3000−6000 to 400−1200 FL/OD_{600}, and clear fluorescence differences between 10 μM and 2.5 mM PA/TPA were observed (Figure 4a,b). Furthermore, the fluorescence ratios of XylS-K38R-L224Q- and XylS-W88C-L224Q-based biosensors relative to the background increased to 2.2- and 3.0-fold in this dynamic range, respectively, which favors the sub-mM detection of PA and TPA (Figure 4c,d). However, the replacement of the original promoter J23114 with other standard promoters did not improve the performance of the engineered whole-cell biosensors (Figure S9).

Whole-Cell Biosensor-Based Evolution of PAE-Degrading Enzymes. As a proof of concept, we used the pCL1920-XylS-K38R-L224Q-*sf*GFP biosensor for the directed evolution of PAE-degrading enzyme *Go*Est15.[8] *Go*Est15 can hydrolyze PAEs into mono-alkyl phthalates, which are subsequently hydrolyzed into PA by *Go*EstM1 (Figure 5a). Here, we inserted the sensing plasmid in the *E. coli* cell to generate a single cell with double plasmids (*Go*Est15-*Go*EstM1/pCL1920-XyIS-K38R-L224Q) for *Go*Est15 evolution (Figure 5b). Homology modeling of *Go*Est15 based on PDB entry 1C7J was conducted and dibutyl phthalate (DBP) was docked into the active-site pocket (Figure S10a,b). Based on the results of homology modeling and molecular docking, a total of 49 residues located around the active site were selected for site-directed saturation mutagenesis (Table S2). Fluorescent screening of the *Go*Est15-mutant libraries (5000 variants) identified several hits that were selected and characterized (Figure S10c). Among them, *Go*Est15-V3 (P306Y/I393V/L78W/F437L/L129I/K76P) was identified and purified (Figure S10d). The specific activity of *Go*Est15-V3 toward DBP and another substrate *p*-nitrophenyl butyrate (*p*NPB), i.e., 4.7 and 54.0 U/$mg_{protein}$, is 2.0- and 2.5-fold higher than that of the wild-type enzyme, respectively. The time-course degradation of 5 mM DBP showed that 96.5% DBP was degraded by *Go*Est15-V3, while only 55% DPB was degraded by the wild-type enzyme in 60 min (Figure 5d), which indicates that the whole biosensor is effective for screening PA-

https://doi.org/10.1021/acssynbio.1c00275
ACS Synth. Biol. 2022, 11, 1106−1113

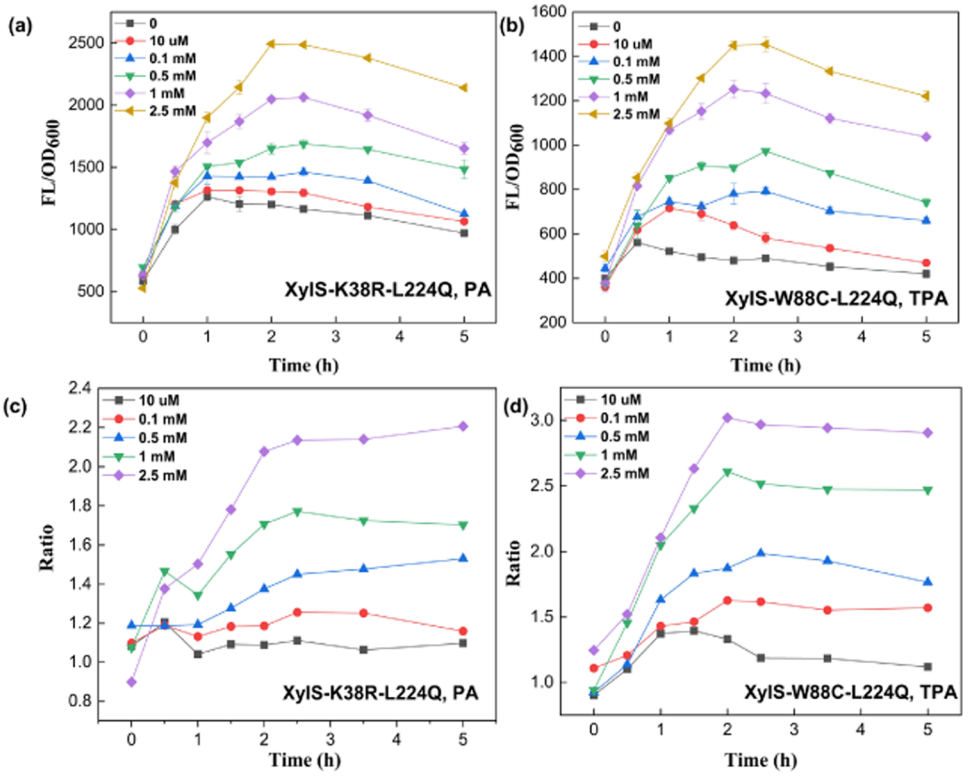

Figure 4. Fluorimetric detection of (a) PA and (b) TPA using engineered XylS-based whole-cell biosensors containing the low-copy pCL1920 plasmid. The corresponding ratios of fluorescence at each time to the background fluorescence are plotted in panels (c) and (d). Each experiment was carried out in three triplicates.

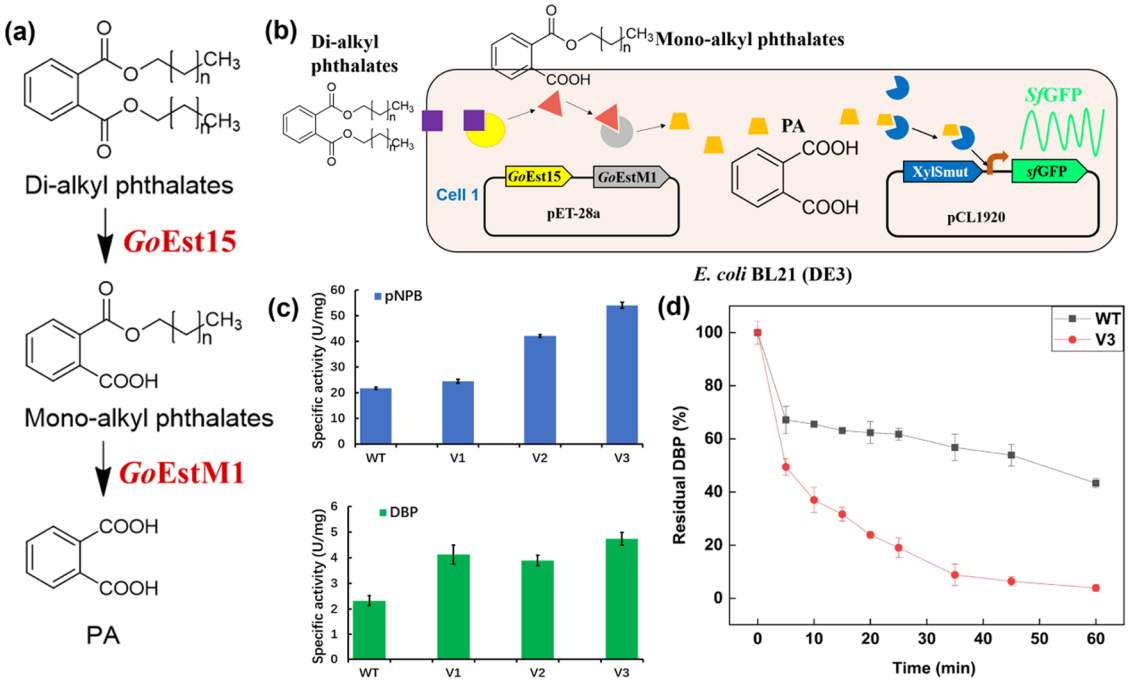

Figure 5. Directed evolution of *Go*Est15. (a) Dual enzyme-catalyzed degradation of PAEs. (b) Illustration of the screening system using a single cell with a double plasmid. (c) Specific activity of the wild-type and various variants of *Go*Est15 toward DBP and *p*NPB. (d) Degradation of 5 mM DBP in 1 mL of phosphate buffer (pH = 7.0) containing 10% dimethylsulfoxide (DMSO) and 0.14 mg of purified enzymes at 30 °C for 60 min. Each experiment was repeated in triplicates.

degrading enzyme variants. We believe that the catalytic performance of *Go*Est15 can be further enhanced by several rounds of iterative evolution. Nevertheless, these results demonstrate the promise of the XylS mutant-based biosensor in the detection of PA for screening of libraries of mutants of PAE-degrading enzymes.

https://doi.org/10.1021/acssynbio.1c00275
ACS Synth. Biol. 2022, 11, 1106−1113

CONCLUSIONS

In conclusion, we created two novel TFs, XylS-K38R-L224Q and XylS-W88C-L224Q, through directed evolution of *P. putida* XylS. These variants can effectively sense as little as 10 μM PA and TPA. As a proof of concept, the biosensor pCL1920-XylS(K38R-L224Q)-*sf*GFP was used for the evolution of *Go*Est15, and a mutant with 2.0- and 2.5-fold enhanced specific activity toward DBP and pNPB was identified. XylS-based whole-cell biosensors directly detect the hydrolysis products of PAE/PET, providing a general screening method for evolving various hydrolases. The detection performance of the biosensor can be further improved by optimization of sensor components and development of more efficient TFs for PA and TPA detection using the methods described in this study.

MATERIALS AND METHODS

General Information. Luria−Bertani (LB) media was used for the culture of *E. coli* cells. PAEs were obtained from Sinopharm Chemical Reagent Co., Ltd. (Shanghai, China). Tryptone and yeast extract were obtained from Oxoid (Hampshire, UK). Other chemicals were purchased from TCI (Japan), Aladdin and Shaoyuan (Shanghai, China). Protein Iso Ni-nitrilotriacetic acid (Ni-NTA) resin was supplied by Trans Gen Biotech (Beijing, China). Ultrafiltration tubing (15 mL/30 kDa) was obtained from Millipore (Shanghai, China). All other reagents were of analytical grade unless otherwise stated. Primers were synthesized by Generay Biotech (Shanghai, China).

Construction of the *E. coli*-pUC57-XylS-*sf*GFP Sensor. The nucleic acid sequence of the transcription factor XylS and its promoter Pm and terminator were handed over to the company for synthesis and synthesized on the pUC57 plasmid and then the recombinant plasmid pUC57-XylS was obtained. During sequence synthesis, *Xho* I and *BamH* I restriction sites were designed at both ends of *sf*GFP. The original *sf*GFP sequence in the laboratory and recombinant plasmid were subjected to double digestion with *Xho* I and *BamH* I, ligated with T4 ligase at 16 °C for 8 h, and the ligation solution was transformed into *E. coli* BL21 (DE3) cells to obtain the *E. coli* biosensor pUC57-XylS-*sf*GFP.

Fluorimetric Detection of PA and TPA with Biosensors in Shaking Flasks. The fluorimetric detection of PA and TPA with the wild-type and mutated biosensors followed the same protocol. Typically, *E. coli* BL21 (DE3) harboring the recombinant plasmid of pUC57-XylS-*sf*GFP was grown overnight at 37 °C in LB medium containing 100 μg/mL ampicillin in 4 mL test tubes. The culture was then inoculated (1% v/v) to 100 mL of LB media in shaking flasks at 37 °C and 220 rpm. When OD_{600} of cells reached 0.6, PA/TPA of different concentrations were added in the culture. For each experiment, samples were collected from three different shaking flasks at different time periods and centrifuged for 1 min at 12 000 rpm. The precipitated cells were resuspended in ddH_2O, and samples of 200 μL were taken in the microplate reader (BioTek, Synergy H1) for measurement of fluorescence intensity (λ_{Ex} = 488 nm, λ_{Em} = 515 nm) and cell density (OD_{600}). The ratio of fluorescence intensity to OD_{600} in each well was calculated and the mean values and errors were obtained.

Directed Evolution of XylS. The recombination plasmids containing XylS gene were used as the template for random mutagenesis. $MnCl_2$ (0.25 mM) was added to the PCR system for obtaining the desired mutagenesis rate (ca. 1−2 amino acid mutations per protein). The amplified PCR products were extracted, digested with *Eco*R I and *Hin*d III and ligated into the *Eco*R I and *Hin*d III sites of pUC57, then transformed into chemical competent *E. coli* BL21 (DE3) cells, and plated on an LB agar plate containing 100 μg/mL ampicillin. The colonies were picked with sterile toothpicks to inoculate in 300 μL of LB media containing 100 μg/mL ampicillin in 96-well plates. The mutants were grown overnight at 37 °C prior to inoculation in 550 μL of LB in new 96-well plates. The plates were incubated at 37 °C for 2 h and then PA/TPA was added and cultured at 37 °C for 8−10 h. A volume of 50 μL of the sample from each well was mixed with 150 μL of ddH_2O and then transferred to a new microtiter plate for the measurement of OD_{600} and fluorescence using a microplate spectrophotometer (BioTek, Synergy H1). The mutants with large differences in FL/OD_{600} compared with the wild-type were selected for shaking flask rescreening, and the best mutants were characterized by subsequent experiments.

Single Cell Analysis with Confocal Fluorescence Microscopy and FACS. Whole-cell biosensors harboring pUC57-XylS-*sf*GFP and pUC57-$XylS_{mut}$-*sf*GFP were cultured following the above protocol. The collected cells were resuspended in 100 mM PBS buffer (pH 7.0) and diluted to OD_{600} 0.1 for determination. For confocal microscopy, Nikon A1R (Nikon, Japan) equipped with a 488 nm exciter was used for fluorescence imaging. Cell samples of 5 μL were pipetted on a glass slide covered with a coverslip and sealed with oil around the slide. The glass slide was placed on the loading platform, and a 100× lens was selected for imaging. The FACS (CytoFLEX LX, Beckman Coulter) utilizing the software CytExpert was used to analyze single *E. coli* cells with PA and TPA induction. The FACS housed a laser/photomultiplier system with excitation at 488 nm and emission at 513 nm. The software sorting accuracy was set to single events and the event rate was adjusted to around 1000 events per second (EPS). The collected cells were resuspended in 100 mM PBS buffer (pH 7.0). The cell density was diluted to 10^7/mL and the samples were injected at 10 μL/min.

Structural Analysis. Homology-based models of *Go*Est15 were constructed using SWISS-MODEL (http://swissmodel.expasy.org/). The template for modeling was the esterase Pnb Esterase 56c8 from *Bacillus subtilis* (PDB code: 1C7J), which shared 37% identity with *Go*Est15. The *Go*Est15 was used as a rigid receptor for docking of DBP and DEHP using AutoDock4.0. The figure was generated using the program PyMOL.

Directed Evolution of *Go*Est15. Residues lining in the substrate binding pocket of *Go*Est15 were targeted, and a library was generated by NNK-based saturation mutagenesis. The site-saturation mutagenesis (1400 clones screened) included 14 residues (L77, T81, G117, G118, A119, E203, A205, Y234, P306, L347, F348, K350, I393, G433). The recombination plasmid containing *Go*Est15 used as the template was amplified by PCR with NNK codon degeneracy. The resulting PCR products were digested with *Dpn* I (20 U) at 37 °C for 3 h and was next transformed into chemical competent *E. coli* BL21 (DE3) cells containing the pCL1920-XylS(K38R-L224Q)-sfGFP biosensor and plated on an LB agar plate containing 50 μg/mL kanamycin and 100 μg/mL streptomycin. Then, single clones were picked up and cultured to express the mutated enzyme in deep well plates and induced

https://doi.org/10.1021/acssynbio.1c00275
ACS Synth. Biol. 2022, 11, 1106−1113

with 200 μM IPTG for 4 h at 16 °C. After IPTG induction, DBP (5 mM) was added to each deep well plate and reactions were carried out for 4 h at 35 °C. Selection of positive mutants was based on the FL/OD_{600} value.

Purification of *Go*Est15 Variants. *E. coli* BL21 (DE3) cells harboring pET28a-*Go*Est15-*Go*EstM1 were grown overnight at 37 °C in LB medium containing 50 μg/mL kanamycin. The overnight culture was then inoculated to 100 mL of LB at 37 °C and 220 rpm. The temperature was then lowered to 16 °C and protein expression was induced with 0.1 mM IPTG until OD_{600} reached 0.6. The culture was grown for 24 h before harvest. After centrifugation, the cells were resuspended in buffer A (20 mM phosphate buffer, 500 mM NaCl, 10 mM imidazole, 5 mM DTT, pH 7.4), disrupted by sonication, and the cell lysate was centrifuged (7500 rpm) for 60 min. The supernatant was loaded on a 2 mL Ni-NTA resin. The retained protein was eluted with a linear gradient from buffer A to buffer B (20 mM phosphate buffer, 500 mM NaCl, 500 mM imidazole, 5 mM DTT, pH 7.4). Purified proteins were exchanged into buffer C (20 mM phosphate buffer, 200 mM NaCl, pH 7.4) using an Ultra-4 centrifugal filter with 30 kDa cut-off (Millipore) and stored with 20% glycerol (v/v) at −80 °C.

Degradation of DBP by Purified *Go*Est15. The reaction mixture (1 mL) containing 100 mM PBS (pH 7.0), 5 mM DBP (dissolved in 10% DMSO), and 0.14 mg of enzyme was incubated for 1 h at 30 °C. Samples were taken at defined time intervals and subjected to HPLC analysis.

HPLC Analysis. All samples dissolved in methanol were passed through a 0.22 μm filter membrane. HPLC separation was performed on a Shimadzu LC-2010A HT apparatus equipped with a Hypersil ODS2-C18 column (5.0 μm, 4.6 × 250 mm). The mobile phase, 5% H_2O and 95% methanol (vol %), was run at a flow rate of 0.8 mL/min, and the oven temperature was 30 °C. The eluent was monitored by absorbance at 254 nm.

■ ASSOCIATED CONTENT

Supporting Information

The Supporting Information is available free of charge at https://pubs.acs.org/doi/10.1021/acssynbio.1c00275.

Construction of whole-cell biosensors (Figure S1), characterization of the wild-type biosensor (Figure S2), characterization of various XylS variants (Figures S3−S6), effector scope of the developed biosensors (Figures S7 and S8), promoter engineering (Figure S9), characterization and structural analysis of *Go*Est15 (Figure S10), PA/TPA detection by XylS variants (Table S1), and primers (Table S2) constructed in this study (PDF)

■ AUTHOR INFORMATION

Corresponding Author

Yunpeng Bai − *State Key Laboratory of Bioreactor Engineering, East China University of Science and Technology, Shanghai 200237, China;* orcid.org/0000-0002-6973-581X; Email: ybai@ecust.edu.cn

Authors

Jiawei Li − *State Key Laboratory of Bioreactor Engineering, East China University of Science and Technology, Shanghai 200237, China*

Mario Roque Huanca Nina − *State Key Laboratory of Bioreactor Engineering, East China University of Science and Technology, Shanghai 200237, China*

Xiaoyan Zhang − *State Key Laboratory of Bioreactor Engineering, East China University of Science and Technology, Shanghai 200237, China*

Complete contact information is available at: https://pubs.acs.org/10.1021/acssynbio.1c00275

Author Contributions

‡J.L., M.R.H.N., and X.Z. contributed equally to this work. The manuscript was written through contributions of all authors.

Notes

The authors declare no competing financial interest.

■ ACKNOWLEDGMENTS

This work was financially sponsored by the National Key Research and Development Program of China (2016YFA0204300), the National Natural Science Foundation of China (No. 22078096), and the Natural Science Foundation of Shanghai (18ZR1409900).

■ REFERENCES

(1) Amaral-Zettler, L. A.; Zettler, E. R.; Mincer, T. J. Ecology of the plastisphere. *Nat. Rev. Microbiol.* **2020**, *18*, 139−151.

(2) Hale, R. C.; Seeley, M. E.; La Guardia, M. J.; Mai, L.; Zeng, E. Y. A global perspective on microplastics. *J. Geophys. Res.: Oceans* **2020**, *125*, No. e2018JC014719.

(3) Vollmer, I.; Jenks, M. J. F.; Roelands, M. C. P.; White, R. J.; Harmelen, T.; Wild, P.; Laan, G. P.; Meirer, F.; Keurentjes, J. T. F.; Weckhuysen, B. M. Beyond mechanical recycling: giving new life to plastic waste. *Angew. Chem., Int. Ed.* **2020**, *59*, 15402−15423.

(4) Guzzetti, E.; Sureda, A.; Tejada, S.; Faggio, C. Microplastic in marine organism: environmental and toxicological effects. *Environ. Toxicol. Pharmacol.* **2018**, *64*, 164−171.

(5) Gao, D. W.; Wen, Z. D. Phthalate esters in the environment: Acritical review of their occurrence, biodegradation, and removal during wastewater treatment processes. *Sci. Total Environ.* **2016**, *541*, 986−1001.

(6) Abdel daiem, M. M.; Rivera-Utrilla, J.; Ocampo-Perez, R.; Mendez-Diaz, J. D.; Sanchez-Polo, M. Environmental impact of phthalic acid esters and their removal from water and sediments by different technologies−a review. *J. Environ. Manage.* **2012**, *109*, 164−178.

(7) Zhang, W.; Li, X.; Guo, C. Spatial distribution, historical trend, and ecological risk assessment of phthalate esters in sediment from Taihu Lake, China. *Environ. Sci. Pollut. Res.* **2021**, *28*, 25207−25217.

(8) Huang, H.; Zhang, X. Y.; Chen, T. L.; Zhao, Y. L.; Xu, D. S.; Bai, Y. P. Biodegradation of structurally diverse phthalate esters by a newly identified esterase with catalytic activity toward di(2-ethylhexyl) phthalate. *J. Agric. Food Chem.* **2019**, *67*, 8548−8558.

(9) Yoshida, S.; Hiraga, K.; Takehana, T.; Taniguchi, I.; Yamaji, H.; Maeda, Y.; Toyohara, K.; Miyamoto, K.; Kimura, Y.; Oda, K. A bacterium that degrades and assimilates poly(ethylene terephthalate). *Science* **2016**, *351*, 1196−1199.

(10) Tournier, V.; Topham, C. M.; Gilles, A.; David, B.; Fologas, C.; Moya-Leclair, E. M.; Kamionka, E.; Desrousseaux, M. L.; Texier, H.; Gavalda, S.; Cot, M.; Guémard, E.; Dalibey, M.; Nomme, J.; Cioci, G.; Barbe, S.; Chateau, M.; André, I.; Duquesne, S.; Marty, A. An engineered PET depolymerase to break down and recycle plastic bottles. *Nature* **2020**, *580*, 216−219.

(11) Taniguchi, I.; Yoshida, S.; Hiraga, K.; Miyamoto, K.; Kimura, Y.; Oda, K. Biodegradation of PET: current status and application aspects. *ACS Catal.* **2019**, *9*, 4089−4105.

(12) Perpetuo, E.-A.; Esther, C.; Karolski, B.; Nascimento, C. Biodegradation of diethyl-phthalate (DEP) by halotolerant bacteria

isolated from an estuarine environment. *Biodegradation* **2020**, *31*, 331−340.
(13) Carniel, A.; Valoni, R.; Junior, J.-N.; Gomes, A.-C.; Castro, A.-M.-D. Lipase from Candida antarctica (CALB) and cutinase from *Humicola insolens* act synergistically for PET hydrolysis to terephthalic acid. *Proc. Biochem.* **2017**, *59*, 84−90.
(14) Barth, M.; Honak, A.; Oeser, T.; Wei, R.; Belisário-Ferrari, M.-R.; Then, J.; Schmidt, J.; Zimmermann, W. A dual enzyme system composed of a polyester hydrolase and a carboxylesterase enhances the biocatalytic degradation of polyethylene terephthalate films. *Biotechnol. J.* **2016**, *11*, 1082−1087.
(15) Kan, Y. Y.; He, L. H.; Luo, Y. Z.; Bao, R. *Is*PETase Is a novel biocatalyst for poly(ethylene terephthalate) (PET) hydrolysis. *ChemBioChem* **2021**, *22*, 1706−1716.
(16) Austin, H. P.; Allen, M. D.; Bonohoe, B. S.; et al. Characterization and engineering of a plastic-degrading aromatic polyesterase. *Proc. Natl. Acad. Sci. U.S.A.* **2018**, *115*, E4350−E4357.
(17) Ma, Y.; Yao, M. D.; Li, B. Z.; Ding, M. Z.; He, B.; Chen, S.; Zhou, X.; Yuan, Y. J. Enhanced poly (ethylene terephthalate) hydrolase activity by protein engineering. *Engineering* **2018**, *4*, 888−893.
(18) Meng, X. X.; Yang, L. X.; Liu, H. Q.; Li, Q. B.; Xu, G. S.; Zhang, Y.; Guan, F. F.; Zhang, Y. H.; Zhang, W.; Xu, N. F.; Tian, J. Protein engineering of stalbe *Is*PETase for PET plastic degradation by Premuse. *Int. J. Biol. Macromol.* **2021**, *180*, 667−676.
(19) Knott, B. C.; Erickson, E.; Allen, M. D.; et al. Characterization and engineering of a two-enzyme system for plastic depolymerization. *Proc. Natl. Acad. Sci. U.S.A.* **2020**, *117*, E25476−E25485.
(20) Chen, C. C.; Han, X.; Ko, T. P.; Liu, W. D.; Guo, R. T. Structural studies reveal the molecular mechanism of PETase. *FEBS J.* **2018**, *285*, 3717−3723.
(21) Berselli, A.; Ramos, M. J.; Menziani, M. C. Novel Pet-degrading enzymes: structure-function from a computational perspective. *ChemBioChem* **2021**, *22*, 2032−2050.
(22) Cui, Y. L.; Chen, Y. C.; Liu, X. Y.; Dong, S. J.; Tian, Y. E.; Qiao, Y. X.; Mitra, R.; Han, J.; Li, C. L.; Han, X.; Liu, W. D.; Chen, Q.; Wei, W. Q.; Wang, X.; Du, W. B.; Tang, S. Y.; Xiang, H.; Liu, H. Y.; Liang, Y.; Houk, K. N.; Wu, B. Computational redesign of a PETase for plastic biodegradation under ambient condition by the GRAPE strategy. *ACS Catal.* **2021**, *11*, 1340−1350.
(23) Chen, C. C.; Han, X.; Li, X.; Jiang, P. C.; Niu, D.; Ma, L. X.; Liu, W. D.; Li, S. Y.; Qu, Y. Y.; Hu, H. B.; Min, J.; Yang, Y.; Zhang, L. L.; Zeng, W.; Huang, J. W.; Dai, L. H.; Guo, R. T. General features to enhance enzymatic activity of poly(ethylene terephthalate) hydrolysis. *Nat. Catal.* **2021**, *4*, 425−430.
(24) Pirillo, V.; Pollegioni, L.; Molla, G. Analytical methods for the investigation of enzyme-catalyzed degradation of polyethylene terephthalate. *FEBS J.* **2021**, *288*, 4730−4745.
(25) Yang, X. F.; Guo, X. Q. Fe(II)-EDTA chelateinduced aromatic hydroxylation of terephthalate as a new method for the evaluation of hydroxyl radical scavenging ability. *Analyst* **2001**, *126*, 928−932.
(26) Wei, R.; Oeser, T.; Billig, S.; Zimmermann, W. A high-throughput assay for enzymatic polyester hydrolysis activity by fluorimetric detection. *Biotechnol. J.* **2012**, *7*, 1517−1521.
(27) Chaves, M. R. B.; Lima, M. L. S. O.; Malafatti-Picca, L.; De Angelis, D. A.; De Castro, A. M.; Valoni, E.; Marsaioli, A. J. A practical fluorescence-based screening protocol for polyethylene terephthalate degrading microorganisms. *J. Braz. Chem. Soc.* **2018**, *29*, 1278−1285.
(28) Li, J. W.; Zhang, X. Y.; Wu, H.; Bai, Y. P. Transcription factor engineering for high-throughput strain evolution and organic acid bioproduction: a review. *Front. Bioeng. Biotechnol.* **2020**, *8*, No. 98.
(29) Choi, S. L.; Rha, E.; Lee, S. J.; Kim, H.; Kwon, K.; Jeong, Y. S. Y.; Rhee, H.; Song, J. J.; Kim, H. S.; Lee, S. G. Toward a generalized and high-throughput enzyme screening system based on artificial genetic circuits. *ACS Synth. Biol.* **2014**, *3*, 163−171.
(30) Kwon, K. K.; Yeom, S. J.; Choi, S. L.; Rha, E.; Lee, H.; Kim, H.; Lee, D. H.; Lee, S. G. Acclimation of bacterial cell state for high-throughput enzyme engineering using a DmpR-dependent transcriptional activation system. *Sci. Rep.* **2020**, *10*, No. 6091.
(31) Kwon, K. K.; Lee, D. H.; Kim, S. J.; Choi, S. L.; Rha, E.; Yoem, S. J.; Subhadra, B.; Lee, J.; Jeong, K. J.; Lee, S. G. Evolution of enzymes with new specificity by high-throughput screening using DmpR-based genetic circuits and multiple flow cytometry rounds. *Sci. Rep.* **2018**, *8*, No. 2659.
(32) Zhang, Y. Y.; Zhang, X. Y.; Cheng, H.; Huanca Nina, M. R.; Bai, Y. P. Reshaping the active pocket of promiscuous lactonases for degrading bulky organophosphate flame retardants. *Chem. Commun.* **2021**, *57*, 6475−6478.
(33) Raghavan, S.-S.; Chee, S.; Li, J.; Poschmann, J.; Ghadessy, F.-J. Development and application of a transcriptional sensor for detection of heterologous acrylic acid production in *E. coli*. *Microb. Cell Fact.* **2019**, *18*, 139−150.
(34) FM Machado, L.; Currin, A.; Dixon, N. Directed evolution of the PcaV allosteric transcription factor to generate a biosensor for aromatic aldehydes. *J. Biol. Eng.* **2019**, *13*, 91−105.
(35) Kim, S. K.; Kim, S.; Subhadra, B.; Woo, S. G.; Lee, S. G.; et al. A Genetically encoded biosensor for monitoring isoprene production in engineered *Escherichia coli*. *ACS Synth. Biol.* **2018**, *7*, 2379−2390.
(36) Liu, C.; Zhang, B.; Liu, Y. M.; Yang, K. Q.; Liu, S. J. New intracellular shikimic acid biosensor for monitoring shikimate synthesis in *Corynebacterium glutamicum*. *ACS Synth. Biol.* **2018**, *7*, 591−601.
(37) Dabirian, Y.; Li, X.; Chen, Y.; David, F.; Siewers, V.; et al. Expanding the Dynamic range of a transcription factor-based biosensor in *Saccharomyces cerevisiae*. *ACS. Synth. Biol.* **2019**, *8*, 1968−1975.
(38) Sasoh, M.; Masai, E.; Ishibashi, S.; Hara, H.; Kamimura, N.; Miyauchi, K.; Fukuda, M. Characterization of the terephthalate degradation genes of *Comamonas* sp. Strain E6. *Appl. Environ. Microbiol.* **2006**, *72*, 1825−1832.
(39) Kok, R. G.; D'Argenio, D. A.; Ornston, L. N. Mutation analysis of PobR and PcaU, closely related transcriptional activators in *Acinetobacter*. *J. Bacteriol.* **1998**, *180*, 5058−5069.
(40) Jha, R. K.; Kern, T. L.; Kim, Y. C.; Tesar, C.; Jedrzejczak, R.; Joachimiak, A.; Strauss, C. E. M. A microbial sensor for organophosphate hydrolysis exploiting an engineered specificity switch in a transcription factor. *Nucleic Acids Res.* **2016**, *44*, 8490−8500.
(41) Mahr, R.; Frunzke, J. Transcription factor-based biosensors in biotechnology: current state and future prospects. *Appl. Microbiol. Biotechnol.* **2016**, *100*, 79−90.
(42) Figueiredo, R.; Llerena, J. P. P.; Kiyota, E.; Ferreira, S. S.; Cardeli, B. R.; Souza, S. C.; Brito, M. D. S.; Sodek, L.; Cesarino, I.; Mazzafera, P. The sugarcane ShMYB78 transcription factor activates suberin biosynthesis in *Nicotiana benthamiana*. *Plant Mol. Biol.* **2020**, *104*, 411−427.
(43) Majewski, P.; Gutowska, A.; Sacha, P.; Schneiders, T.; Tryniszewska, E. Expression of AraC/XylS stress response regulators in two distinct carbapenem-resistant *Enterobacter cloacae* ST89 biotypes. *J. Antimicrob. Chemother.* **2020**, *75*, 1146−1150.
(44) Belmont-Monroy, L.; Saitz-Rojas, W.; Soria-Bustos, J.; Mickey, A. S.; Sherman, N. E.; Orsburn, B. C.; Ruiz-Perez, F.; Santiago, A. E. Characterization of a novel AraC/XylS-regulated family of N-acyltransferases in pathogens of the order Enterobacterales. *PLoS Pathog.* **2020**, *16*, No. e1008776.
(45) Ogawa, Y.; Katsuyama, Y.; Ueno, K.; Ohnishi, Y. Switching the ligand specificity of the biosensor XylS from meta to para-toluic acid through directed evolution exploiting a dual selection system. *ACS Synth. Biol.* **2019**, *8*, 2679−2689.
(46) Monteiro, L. M. O.; Arruda, L. M.; Sanches-Medeiros, A.; Martins-Santana, L.; Alves, L. F.; Defelipe, L.; Turjanski, A. G.; Guazzaroni, M. E.; Lorenzo, V.; Silva-Rocha, R. Reverse engineering of an aspirin-responsive transcriptional regulator in *Escherichia coli*. *ACS Synth. Biol.* **2019**, *8*, 1890−1900.

https://doi.org/10.1021/acssynbio.1c00275
ACS Synth. Biol. 2022, 11, 1106−1113